2014

A New Model for the Analysis of Performance in Evacuated Tube Solar Collectors

Ahmed Aboulmagd
Cairo University, Egypt, a.aboulmagd@eng.cu.edu.eg

Andrea Padovan
University of Padova, Italy, a.padovan@unipd.it

Rejane De Césaro Oliveski
University of Vale do R, decesaro@unisinos.br

Davide Del Col
University of Padova, Italy, davide.delcol@unipd.it

A NEW MODEL FOR THE ANALYSIS OF PERFORMANCE IN EVACUATED TUBE SOLAR COLLECTORS

Ahmed Aboulmagd[1], Andrea Padovan[2], Rejane De Césaro Oliveski[3], Davide Del Col[2*]

[1]Cairo University, Faculty of Engineering, Mechanical Power Dept., Cairo, Egypt
a.aboulmagd@eng.cu.edu.eg

[2]Università di Padova, Dipartimento di Ingegneria Industriale, Via Venezia 1, Padova, Italy
davide.delcol@unipd.it; a.padovan@unipd.it

[3]University of Vale do Rio dos Sinos, Department of Mechanical Engineering, São Leopoldo, Brazil
decesaro@unisinos.br

*Corresponding Author

ABSTRACT

This paper describes a new model for the performance analysis of evacuated tube solar collectors. The analyzed collector is equipped with truncated compound parabolic reflectors, but the analysis is also extended to the case of collectors without reflectors. An original software is developed under MATLAB environment for the simulation purpose. A novel numerical procedure is implemented to obtain the solution for the nonlinear set of equations representing the mathematical model. In the model, the variation of important parameters is considered in the circumferential, longitudinal and radial directions. The length of the tube, where the heat transfer fluid flows, can be divided into a specified number of segments and the energy analysis is performed for each segment along the tube length in order to obtain the variation of different parameters in the longitudinal direction. The model analyzes separately the optics and the heat transfer in the evacuated tubes and this approach allows to extend the analysis to new configurations. The model can simulate the efficiency curve under steady-state conditions, according to the standard EN 12975-2 (EN 12975-2. Thermal solar systems and components - solar collectors - part 2: test methods. Brussels: CEN; 2006). A comparison with experimental data shows the accuracy of the present model.

1. INTRODUCTION

Solar collectors can provide a useful response to the heat demand in buildings, such as heating of domestic water and spaces. Beside the heating application, there is also need to meet the increasing energy consumption due to the summer air conditioning. In the latter application, solar collectors can supply heat to absorption machines, where the temperature levels required for the input heat are higher than 80 °C. In the work of Zambolin and Del Col (2010), an experimental comparison of thermal performance of flat plate and evacuated tube solar collectors was performed. The efficiency of the evacuated tube collector is higher when the reduced temperature difference exceeds 0.035 m^2 K/W. For instance, for a global solar irradiance of 1000 W/m^2, the performance of the evacuated tube collector is higher than that for the flat plate one when the temperature difference between heat transfer fluid and ambient air is higher than 35 K. If ambient air temperature is 5 °C (winter case), such value of reduced temperature difference occurs when the solar collector produces heat at 40 °C, which is suitable for space heating with radiant panel systems. If ambient air temperature is 25 °C (summer case), such value of reduced temperature difference occurs when the solar collector produces heat at a temperature higher than 60 °C, so evacuated tube collectors can be more suitable for solar cooling. The evacuated tube collectors are subdivided in two main types. The first type is the direct flow collector where the heat transfer liquid is pumped in the tubes. The second type consists of heat pipes inside vacuum sealed glass tubes. In most of cases, both types of collector are equipped with a CPC (Compound Parabolic Concentrator) to optimize the collection of solar radiation. Among the direct through flow types, the U-tube evacuated tube solar collector appears to be a well-developed type of collector. Installations of evacuated tube collectors without CPC are also possible in case of specific requirements in building designs. Theoretical and experimental research works are done on the optical and thermal performance of the evacuated tube solar collector

with U-tube, as reported in Table 1. As compared to the models discussed in Table 1, the present paper introduces a new detailed nonlinear model for evacuated tube solar collectors where a more comprehensive optical and thermal analysis is proposed. The variation of the temperature along both the circumferential (fin) and the longitudinal (tube) directions is considered in the present model. Using experimental data obtained by Zambolin and Del Col (2012) for this type of collector, a validation is done to reveal the accuracy of the present model either with or without external CPC reflectors. Accurate modeling and simulation of this type of collectors is highly recommended to fully assess the performance of the collectors already available in the market and propose improved designs, for example, with higher concentration ratio to get more benefits particularly at higher levels of operating temperature.

Table 1: Summary of some previous works on evacuated tube collectors with U-tube.

Harding *et al.* (1985)	• Experimental and calculation procedures are used to obtain the equation for the instantaneous efficiency. • Effect of wind velocity is neglected. • Experimental data of optical efficiency are reported. • Mathematical model of optical efficiency is not described.
Ma *et al.* (2010)	• One-dimensional (circumferential direction) model for thermal performance of the individual glass evacuated tube solar collector is presented. • $h_{p-g,cond}$, $h_{g-a,conv}$ and $h_{f,conv}$ are constants in the model. • No modeling for optical efficiency is done.
Liang *et. al.* (2011)	• One-dimensional (longitudinal direction) model for thermal performance of filled type evacuated tube solar collectors is presented. • Experimental tests are conducted to validate the model. • $h_{g-a,rad}$ and $h_{g-a,conv}$ are constants in the model. • Optical efficiency effect is considered as the simple transmittance-absorbtance product.
Zambolin and Del Col (2012)	• Based on the EN 12975-2 (2006), experimental efficiency is measured for the collectors both with and without external CPC.

2. DESCRIPTION OF THE EVACUATED TUBE COLLECTOR

The receiver consists of a copper U-tube inside a glass vacuumed tube. The copper tube is surrounded by a cylindrical aluminum fin pressed on it, which has the role of enhancing the heat transfer area between the inner glass absorber surface and the U-tube. Fluid flow in the collector is represented in Fig. 1. The working fluid enters the collector inlet pipe, then it is evenly distributed to the U-tubes, absorbs heat and, at the end, it is returned to the outlet header pipe (Soriga and Neaga, 2012). Fig. 2 shows a scheme of the evacuated tube provided with the truncated compound parabolic reflector. Part of the solar radiation falls directly on the absorber surface, while the rest is reflected by the CPC on the absorber glass tube. The outer cylindrical glass transmits the rays to the inner glass tube, which conducts the energy to the absorber fin. The energy transformed into heat is conducted by the fin to the copper U-tube and finally absorbed by the working fluid, which is water in this case. The detailed illustration of the evacuate tube and its cross section view are given in Fig. 3. Table 2 gives the details of the analytical model parameters considered in the present study for the glass evacuated tube solar collector.

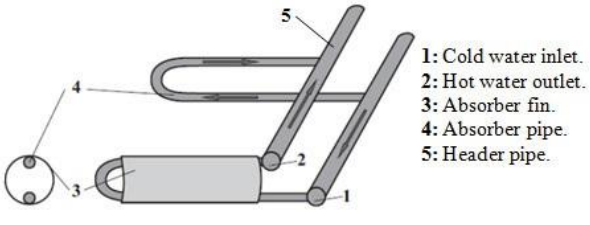

Figure 1: Fluid flow in the collector.

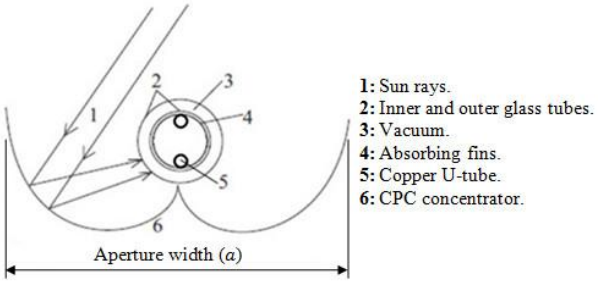

Figure 2: Evacuated tube collector with CPC.

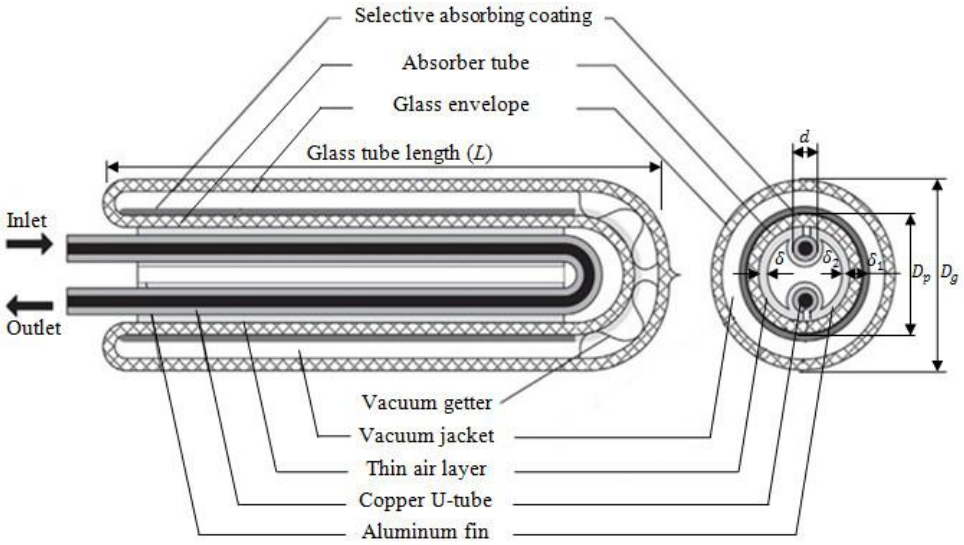

Figure 3: Illustration of the glass evacuated tube solar collector with U-tube.

Table 2: Computational parameters for the evacuated tube solar collector.

Absorbing coating	Absorptivity [-]	0.94
	Emissivity [-]	0.06
Outer glass envelope and absorber glass tube	Outer diameter of glass envelope [m]	0.058
	Outer diameter of absorber tube [m]	0.047
	Glass tube length [m]	1.56
	Aperture width [m]	0.1105
	Thickness of glass [m]	0.0016
	Thermal conductivity of glass [W/(m K)]	1.2
	Transmittance of glass [-]	0.92
Aluminum fin	Thickness [m]	0.0008
	Thermal conductivity [W/(m K)]	220
Copper U-tube	Outer diameter [m]	0.0063
	Thickness [m]	0.0005
	Thermal conductivity [W/(m K)]	370
Header section	Outer diameter of the header pipe [m]	0.016
	Outer diameter of the insulation [m]	0.085
Number of glass tubes		20

3. MATHEMATICAL MODEL

The absorbed solar power, *S*, is equal to the incident solar power reduced by optical losses, given by

$$S = \eta_o I A_{ap} \tag{1}$$

where η_o is the optical efficiency and I is the global solar irradiance on the collector plane. The relation for aperture area is $A_{ap} = a \cdot L$ in case of a collector with CPC or $A_{ap} = D_g \cdot L$ in case of without CPC. In addition, the net heat flow rate transferred to the working fluid is equal to the difference between S and the thermal loss due to radiation, conduction and convection. One-dimensional analytical investigation for the fin of a single unit of the glass evacuated tube solar collector is carried out. The analysis also extends to calculate variation of the parameters in radial and longitudinal directions. The following assumptions are used: (a) thermal resistance of the outer glass tube thickness is negligible; (b) perfect vacuum is assumed between the two glass tubes, thus gas conduction is neglected; (c) the heat flux along the circumferential direction is considered constant although, in practice, the heat flux is not evenly distributed; (d) an air layer of an equivalent thickness of 0.5 mm is considered between aluminum fin and the absorber glass tube to model the irregular contact gap, and (e) steady-state conditions are considered with normal

incidence angle of solar radiation. In order to develop a comprehensive mathematical model of the collector, thermal and optical analysis is performed in detail. Fig. 4 shows a schematic of an evacuated tube collector with mechanisms of energy transfer from the absorber tube to glass envelope and from envelope to surroundings. Fig. 5 gives the thermal network associated with the heat transfer process of the collector. Thermal losses occur by conduction from the insulated header pipes of the manifold when the mean fluid temperature (T_f) is above ambient (T_a), and by conduction and radiation from the absorber tube when the mean temperature of the selective absorbing surface (T_p) is above ambient. Heat loss from the absorber is then transferred to the ambient by convection and radiation. All the losses are referred to the absorber. It can be found from Fig. 5 that the absorbed solar power per unit area (S'') is the sum of the net heat flux gained (q_u'') by the working fluid and the thermal losses per unit area of the absorber (q_L'')

$$S'' = q_u'' + q_L'' \tag{2}$$

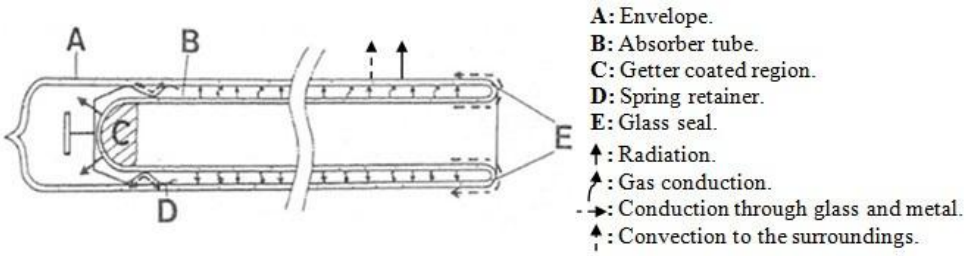

Figure 4: Heat transfer mechanisms in an evacuated tube collector. Adapted from Harding *et al.* (1985).

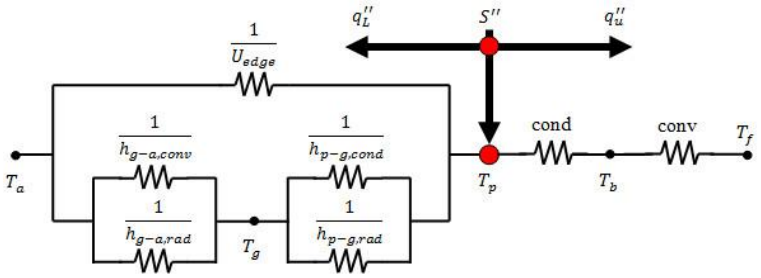

Figure 5: Collector thermal network associated with the heat transfer processes.

3.1 Overall Heat Loss

The thermal losses per unit area of the absorber and the overall loss coefficient (U_L) can be defined, respectively by

$$q_L'' = U_L(T_p - T_a) \tag{3}$$

$$U_L = U_{top} + U_{edge} \tag{4}$$

The edge loss coefficient, U_{edge}, of the header tube can be given by: $U_{edge} = 2\pi\lambda_{ins}/[l \ln(d_{ins,ext}/d_{ins,int})]$, where λ_{ins} is the thermal conductivity of the header pipe insulation, l is the length of the header pipe per one U-tube, $d_{ins,int}$ and $d_{ins,ext}$ are the internal and external diameters of the insulation, respectively. The top loss coefficient from the absorber tube to the ambient, U_{top}, can be written as

$$U_{top} = \left[1/(h_{p-g,cond} + h_{p-g,rad}) + 1/(h_{g-a,conv} + h_{g-a,rad})\right]^{-1} \tag{5}$$

$h_{g\text{-}a,conv}$ is the convection heat transfer coefficient from the outer glass tube to the surroundings. $h_{p\text{-}g,rad}$ is the radiation heat transfer coefficient between the absorber tube and outer glass tube, $h_{p\text{-}g,cond}$ is the conduction heat transfer coefficient by the metal spring retainer between the absorber and glass tube (its calculated value is 1.8 W/(m K)), and $h_{g\text{-}a,rad}$ is the radiation heat transfer coefficient between the outer glass tube and the surroundings. The energy balance gives

$$U_{top}(T_p - T_a) = (h_{p-g,rad} + h_{p-g,cond})(T_p - T_g) = (h_{g-a,conv} + h_{g-a,rad})(T_g - T_a) \tag{6}$$

The radiation heat transfer coefficient between the concentric absorber and outer glass tubes can be given by Eq. (7), Duffie and Beckman (2013).

$$h_{p-g,rad} = \frac{\sigma\epsilon_p}{1+\frac{\epsilon_p D_p}{\epsilon_g D_g}(1-\epsilon_g)}(T_p^2 + T_g^2)(T_p + T_g) \tag{7}$$

where ϵ_p is the emissivity of the selective absorbing coating, ϵ_g is the emissivity of the inner surface of outer glass tube and σ is the Stefan Boltzmann constant. D_p is the outer diameter of absorber tube and D_g is the inner diameter of outer glass tube. Considering the outer glass tube as small convex object surrounded by a large enclosure (the sky), the radiation heat transfer coefficient to the sky, $h_{g-a,rad}$ can be written as

$$h_{g-a,rad} = \sigma\epsilon_g(T_g^2 + T_{sky}^2)(T_g + T_{sky}) \tag{8}$$

The sky temperature is given by: $T_{sky} = T_a - 6$ (Soriga and Neaga, 2012). The convection heat transfer coefficient $h_{g-a,conv} = Nu_a\lambda_a/D_g$, where Nusselt number ($Nu_a$) is given by Eq. (9), Duffie and Beckman (2013).

$$Nu_a = \begin{cases} 0.4 + 0.54Re_a^{0.52}, & 0.1 < Re_a \le 1000 \\ 0.3Re_a^{0.6}, & 1000 < Re_a < 50{,}000 \end{cases} \tag{9}$$

where $Re_a = u_a D_g/v_a$ is the Renolds number of the wind speed (u_a), based on the outer glass tube diameter. Air thermophysical properties are calculated based on the ambient air temperature (T_a).

3.2 Net Heat Gain

Consider the fin and tube configuration as shown in Fig. 6-a, b. The half fin perimeter $W = \pi[D_p - 2(\delta_p + \delta_a)]/2$, the tube diameter is d, thicknesses of absorber tube, air layer, aluminum fin are δ_p, δ_a and δ_{fin}, respectively. For fin length of $(W-d)/2$, an energy balance on an elemental region of width Δx and unit length in the flow direction yields Eq. (10), Ma *et al.* (2010). An analytical procedure is used to solve Eq. (10) with two boundary conditions: $dT/dx|_{x=0} = 0$ and $T|_{x=(W-d)/2} = T_b$ (fin base temperature), resulting in Eq. (11), Duffie and Beckman (2013).

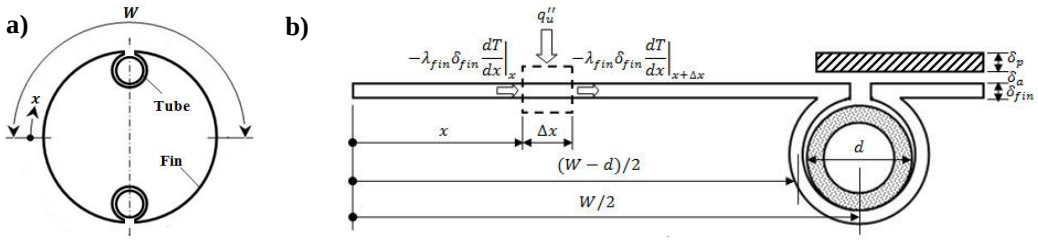

Figure 6: a) Fin and tube configuration. **b)** Energy balance on the circumferential aluminum fin.

$$-\lambda_{fin}\delta_{fin}(dT/dx)_x - \left[-\lambda_{fin}\delta_{fin}(dT/dx)_{x+\Delta x}\right] + q_u''\Delta x = 0 \tag{10}$$

where λ_{fin} is the thermal conductivity of the aluminum fin.

$$T(x) = \frac{cosh\,(mx)}{cosh[m(W-d)/2]}\left(T_b - T_a - \frac{S''}{U_L}\right) + T_a + \frac{S''}{U_L} \tag{11}$$

where $m = \sqrt{U_L/\left[\lambda_{fin}\delta_{fin}(1 + U_L/C_b)\right]}$. Using Eq.(11) and applying Fourier's law at fin base $x = (W-d)/2$ for both right and left sides around the tube, the fin heat flow rate per unit length of the tube is obtained by

$$q_{fin}' = \frac{(W-d)F[S'' - U_L(T_b - T_a)]}{1 + U_L/C_b} \tag{12}$$

$C_b = [\delta_p/\lambda_g + \delta_a/\lambda_a]^{-1}$ is a combined conductance for glass (thermal conductivity of λ_g) and air (thermal conductivity of λ_a) and $F = \tanh[m(W-d)/2]/[m(W-d)/2]$. The heat flow rate collected above the tube region per unit length is given by Eq. (13). The net heat gain per unit length for the collector is given by Eq. (14), which is the sum of Eqs. (12) and (13). This energy must be transferred to the working fluid (mean temperature of T_f), Eq. (15).

$$q_{tube}^{'} = \frac{d[S'' - U_L(T_b - T_a)]}{1 + U_L/C_b} \tag{13}$$

$$q_u^{'} = q_{fin}^{'} + q_{tube}^{'} = \frac{[(W-d)F + d][S'' - U_L(T_b - T_a)]}{1 + U_L/C_b} \tag{14}$$

$$q_u^{'} = \frac{T_b - T_f}{[1/(\pi d_1 h_{f,conv}) + 1/C_B]} \tag{15}$$

$h_{f,conv}$ is the heat transfer coefficient for the flow inside the copper U-tube. C_B is the contact conductance of the fin and the tube. The calculation procedure for C_B is quite not simple because the non-regularity of the gap between contact elements. In the present model, the value for C_B is calculated based on three thermal resistances, resistance of the aluminum fin, the resistance of the copper tube thickness and the contact resistance in between (R')

$$C_B = \left[\frac{\ln(d_2/d)}{2\pi\lambda_{fin}} + R^{'} + \frac{\ln(d/d_1)}{2\pi\lambda_{tube}}\right]^{-1} \tag{16}$$

The contact thermal resistance R' is obtained from Fletcher (1993) assuming medium roughness for the surface of contact. λ_{tube} is the thermal conductivity of the copper tube, d_1 and d are the inner and outer diameters of the copper tube, respectively, and d_2 is the outer diameter of the fin part surrounding the tube. The value of C_B is calculated to be 90.39 W/(m K). The net heat gain for the collector is obtained by solving Eqs. (14) and (15) for T_b

$$q_u^{'} = WF^{'}\left[S'' - U_L(T_f - T_a)\right] \tag{17}$$

$F^{'}$ is collector efficiency factor, given by Eq. (18). For the calculation of T_p, Eq. (19) is used. The convection heat transfer coefficient $h_{f,conv} = Nu_f\lambda_f/d_1$, where Nusselt number ($Nu_f$) is given by Eq. (20), Incropera *et al.* (2007).

$$F^{'} = \frac{1}{WU_L}\left[\frac{1 + U_L/C_b}{U_L[d + (W-d)F]} + \frac{1}{C_B} + \frac{1}{\pi d_1 h_{f,conv}}\right]^{-1} \tag{18}$$

$$q_u^{'} = \frac{T_p - T_f}{\left[\frac{1}{C_b} + \frac{1}{\pi d_1 h_{f,conv}} + \frac{1}{C_B}\right]} \tag{19}$$

$$Nu_f = \begin{cases} 1.86\left(\frac{Re_f Pr_f}{L/d_1}\right)^{1/3}\left(\frac{\mu_f}{\mu_1}\right)^{0.14}, & Re_f \le 2300 \\ \frac{(f/8)(Re_f - 1000)Pr_f}{1 + 12.7(f/8)^{1/2}\left(Pr_f^{2/3} - 1\right)}, & Re_f > 2300 \end{cases} \tag{20}$$

with f = [0.790 $ln(Re_f)$ - 1.64]$^{-2}$, $Re_f = 4\dot{m}_f/(\pi d_1\mu_f)$ is the Renolds number of the fluid based on the inner tube diameter d_1 and Pr_f is the Prandtl number. $\dot{m}_f$ is the mass flow rate of the working fluid per one U-tube. Thermophysical properties of the heat transfer fluid are calculated based on the mean fluid temperature (T_f).

3.3 Parameter Variations along the Tube Length

The glass tube length (L) is divided into a specified, equal, number of divisions (N) each of length (Δy) so that the total number of segments along the U-tube length (y) is 2N, see Fig. 7. The inlet temperature ($T_{f,i}$) at any segment (i) of the U-tube is taken as a boundary condition to produce the temperature value at the exit of the segment ($T_{f,i+1}$). This procedure should continue in an iterative way to obtain variation of parameters for all segments along the entire U-tube. With $T_f = (T_{f,i} + T_{f,i+1})/2$ is the mean fluid temperature for each segment and applying a segment energy balance, Eq. (21) is obtained for the heat flow rate gained for each segment. $c_{p,f}$ is the specific heat of the fluid.

$$q_{u,i} = W(\Delta y)F^{'}\left[S'' - U_L(T_f - T_a)\right] = \dot{m}_f c_{p,f}(T_{f,i+1} - T_{f,i}) \tag{21}$$

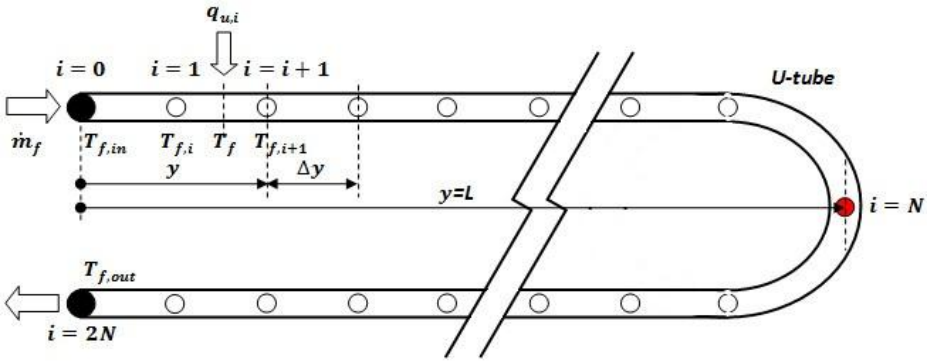

Figure 7: Variation of temperature along the tube length with finite difference notation.

3.4 Optical Efficiency Model

The optical efficiency is defined as the ratio between the absorbed solar power and the total solar power received by the aperture area. In general, the optical efficiency is depending on the optical properties of the materials used (reflectivity, transmissivity and absorptivity), the geometry of the reflector, the space between collector tubes, and solar rays incidence angles. The optical efficiency model used in this study is obtained from Rabl (1976), Eq. (22).

$$\eta_o = (\rho^{\bar{n}} \tau \alpha) \gamma \tag{22}$$

where ρ is the reflectivity of the CPC reflector, τ is the transmissivity of the glass tube and α is the absorptivity of the absorber. In case of a collector without CPC, the product $\rho^{\bar{n}}$ does not exist. The exponent ($\bar{n}$) in the previous equation is the average number of reflections, which depends on the incidence angle of solar radiation (θ) and acceptance half angle of the CPC reflector (θ_c). The behavior of $\bar{n}$ is discussed by Rabl (1975), it decreases with increasing the half acceptance angle and also with decreasing the incidence angle of solar radiation. In the present study, a value of $\bar{n}$ = 0.3 is assumed. The parameter γ is the intercept factor, defined as the fraction of solar radiation accepted by the collector absorber. This factor depends on collector geometry, incidence angle of solar rays and atmospheric conditions. The values of γ are 0.92 and 0.53 for cases with and without CPC, respectively.

3.5 Overall Efficiency

The overall performance of the collector is a combination of optical and thermal performance. This can be expressed by the overall efficiency of the collector, Eq. (23). $A_{ap,tot} = a \cdot L$ is the total aperture area per unit tube for both collectors with or without CPC , $T_{f,in}$ and $T_{f,out}$ are the inlet and outlet temperatures of the U-tube, respectively. Using Eqs. (1), (2), (3) and (23), the overall efficiency can be also given by Eq. (24). A_p is the absorber area. Using Eq.(19), replacing T_p in Eq.(24) with its function in terms of T_f, the resulting overall efficiency is given by Eq. (25).

$$\eta_c = \frac{\dot{m}_f c_{p,f} (T_{f,out} - T_{f,in})}{I \cdot A_{ap,tot}} = \frac{\sum_{i=1}^{2N} q_{u,i}}{I \cdot A_{ap,tot}} \tag{23}$$

$$\eta_c = \eta_o \frac{A_{ap}}{A_{ap,tot}} - U_L \frac{A_p}{A_{ap,tot}} \frac{(T_p - T_a)}{I} \tag{24}$$

$$\eta_c = b_0 - b_1 T_m^* \tag{25}$$

where b_0 and b_1 are nonlinear functions of T_f and $T_m^* = (T_f - T_a)/I$ is the reduced temperature difference.

4. SOLUTION AND RESULTS

Numerical simulation algorithm is implemented in MATLAB to solve the previous nonlinear set of equations forming the collector model. For a specified number of segments taken along the glass tube length of the collector (N = 5 and y = 0 to 2L in Fig. 7), in the following sub sections, simulation results for collectors both with and without CPC will be introduced. Two case studies are considered, one for fixed operating conditions and the other for a wide range of operation. Simulation outputs are provided for the whole collector, which is composed of 20 tubes. A comparison with experimental data is implemented based on the overall performance of the collector.

4.1 A Performance Analysis Case Study

To test the performance of the collector at specific working conditions of T_a = 20 °C, $T_{f,in}$ = 40 °C, $\dot{m}_{f,c}$ = 0.07 kg/s (total mass flow rate for the collector), u_a = 3 m/s and I = 1000 W/m^2, the following simulation outputs are obtained. Figs. 8 and 9 show the variation of local temperatures along the U-tube length for both collectors with and without CPC, respectively. The outer glass tube is fairly constant along tube length, equal to 21 °C. This value is slightly higher than the ambient temperature. Average values of overall heat transfer coefficient, net heat gain, collector efficiency factor and collector efficiencies are given in Table 3 for both collectors with and without CPC.

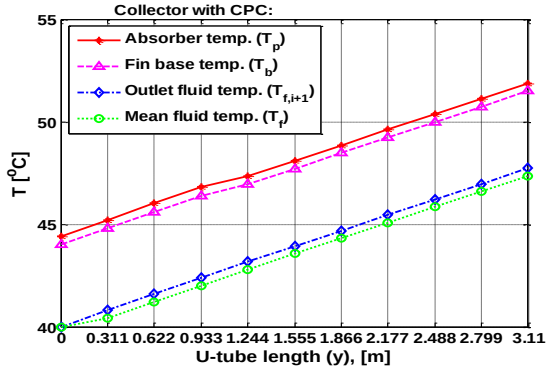

Figure 8: Variation of local temperatures along the U-tube length. Collector with CPC.

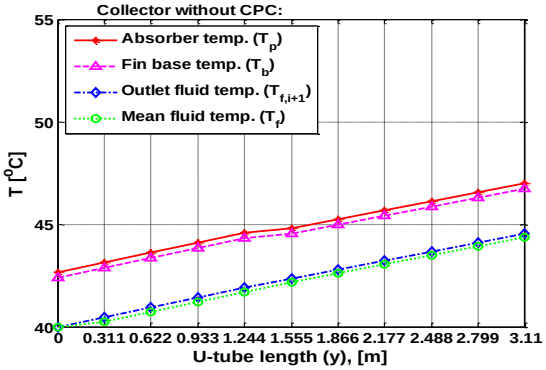

Figure 9: Variation of local temperatures along the U-tube length. Collector without CPC.

Table 3: Average values of different performance parameters for both collectors with and without CPC.

	U_L [W/(m^2 K)]	$q_{u,c}$ (total) [W]	F' [-]	η_{th} [%]	η_o [%]	η_c [%]
with CPC	0.9978	2290	0.9736	85.0	78.4	66.6
without CPC	0.9915	1376	0.9737	83.2	45.8	40.0

4.2 Overall Performance and Comparison to Experimental Data

In this section, the overall performance of the collector at varying ambient and inlet fluid temperatures is introduced. For T_m^* ranging from 0 to 0.06 m^2 K/W and T_a ranging from 5 to 35 °C, the following simulation outputs are obtained. Figs. 10 and 11 introduce the variation of collector overall heat loss coefficient as a function of reduced temperature difference for both collectors with and without CPC, respectively. Figs. 12 and 13 introduce the variation of collector overall efficiency as a function of reduced temperature difference for both collectors with and without CPC at different levels of ambient temperatures. A small effect of ambient temperature on overall heat loss coefficient and efficiency is observed. Thermal (η_{th}), optical (η_o) and overall (η_c) efficiencies of the collector are shown in Figs. 14 and 15 for both collectors with and without CPC, respectively (for T_a = 20 °C). Fig. 16 shows a comparison between numerical simulation output of the present model and the experimental steady-state results obtained by Zambolin and Del Col (2012) for collectors with and without CPC (for T_a = 20 °C). The percentage absolute error between numerical and experimental results at each measurement point is given by Fig. 17.

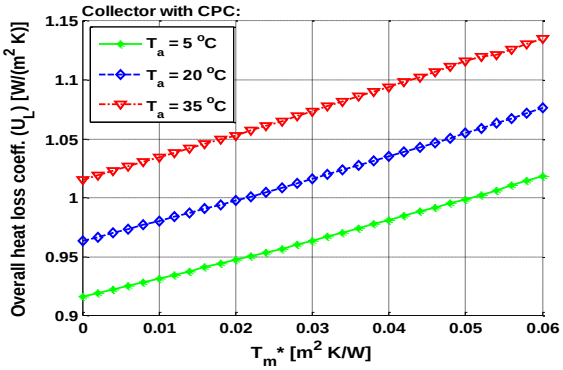

Figure 10: Overall heat loss coefficient vs. reduced temperature difference. Collector with CPC.

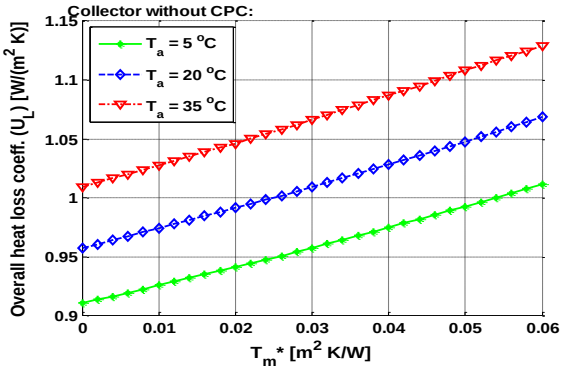

Figure 11: Overall heat loss coefficient vs. reduced temperature difference. Collector without CPC.

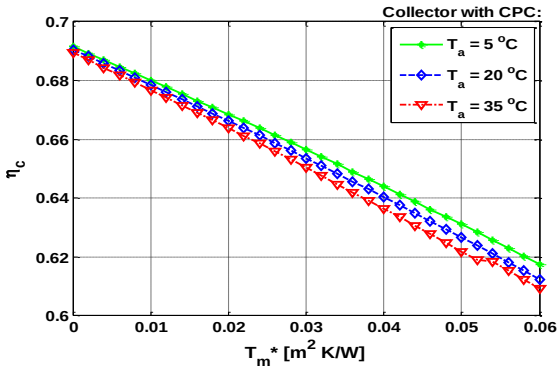

Figure 12: Overall efficiency vs. reduced temperature difference. Collector with CPC.

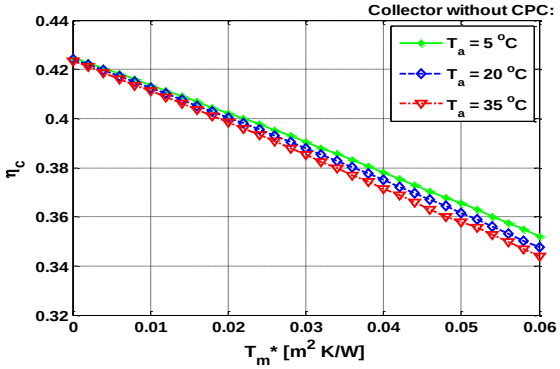

Figure 13: Overall efficiency vs. reduced temperature difference. Collector without CPC.

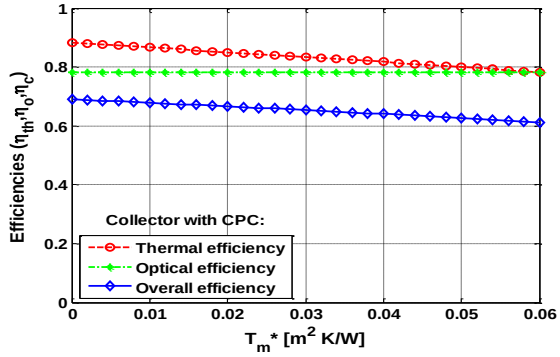

Figure 14: Thermal, optical and overall efficiencies vs. T_m^* (T_a = 20 °C). Collector with CPC.

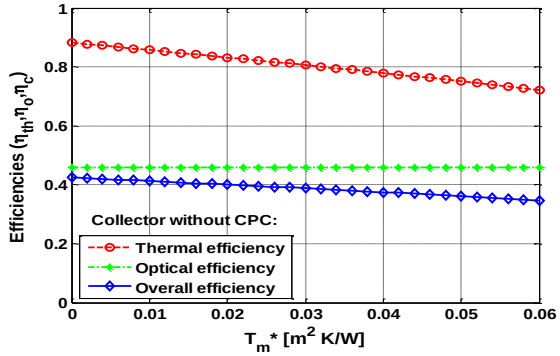

Figure 15: Thermal, optical and overall efficiencies vs. T_m^* (T_a = 20 °C). Collector without CPC.

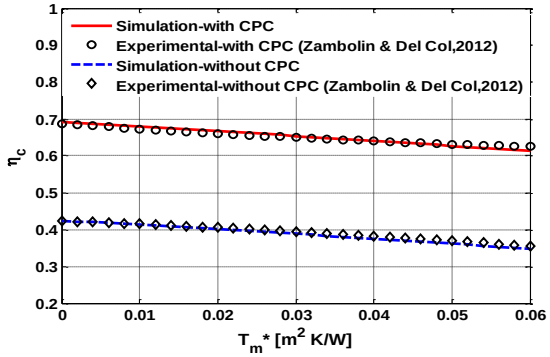

Figure 16: Overall efficiency comparison of simulation and experimental results (T_a = 20 °C).

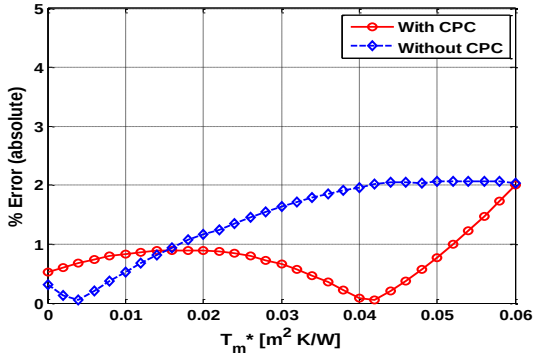

Figure 17: Absolute error (%) between simulation output and experimental results.

5. CONCLUSIONS

A new non-linear model is developed for an evacuated U-tube solar collector with and without CPC reflectors. Regarding the thermal analysis, all the parameters are calculated, so that the model can be extended to different operating conditions and designs. For the proposed optical model, only the parameter "intercept factor (γ)" is estimated, being the rest of the model completely theoretical. Temperature profiles are obtained along circumferential, longitudinal and radial directions of the evacuated tubes. The comparison with experimental data measured at the same conditions shows the good predicting accuracy of the model. For the CPC collector, the overall efficiency is higher than 0.6 even at 0.06 m^2 K/W reduced temperature difference and this is interesting for winter heating and summer cooling applications. For the collector without CPC, the overall efficiency is lower than that of CPC collector, due to the reduced optical performance (Fig. 16). Future work will be aimed at including quasi-dynamic operating conditions in the model to calculate daily heat production.

NOMENCLATURE

A	Area	(m^2)
a	Aperture width	(m)
C	Thermal conductance	W/(m K)
c_p	Specific heat	J/(kg K)
D	Diameter	(m)
d	Copper tube outer diameter	(m)
F'	Collector efficiency factor	(-)
h	Heat transfer coefficient	W/(m^2 K)
I	Total solar irradiance	(W/m^2)
L	Glass tube length	(m)
$\dot{m}$	Mass flow rate	(kg/s)
$\overline{n}$	Average number of reflections	(-)
q	Heat flow rate	(W)
R'	Contact thermal resistance	(m K/W)
S	Absorbed solar power	(W)
T	Temperature (°C); (K) in Eqs. (7) and (8)	
T_m^*	Reduced temperature difference	(m^2 K/W)
U	Overall heat transfer coefficient	W/(m^2 K)
W	Half fin perimeter	(m)

Subscripts

a	ambient air
ap	aperture
b	base
c	collector
f	fluid
g	glass
ins	insulation
L	Loss
o	optical
p	glass absorber
th	thermal
u	useful

Greek Letters

λ	Thermal conductivity	W/(m K)
υ	Kinematic viscosity	(m^2/s)
μ	Dynamic viscosity	kg/(m s)
δ	Thickness	(m)
η	Efficiency	(-)
α	Absorbtivity	(-)
ρ	Reflectivity	(-)
τ	Transmissivity	(-)
γ	Intercept factor	(-)

REFERENCES

Duffie, J.A., Beckman, W.A., 2013, Solar Engineering of Thermal Processes, John Wiley & Sons, Inc., New Jersey.

EN 12975-2: thermal solar systems and components e Solar collectors e Part 2: test methods.

Fletcher, L.S., 1993, Experimental Techniques for Thermal Contact Resistance Measurements, *Experimental Heat Transfer, Fluid Mechanics and Thermodynamics*, p. 195-206.

Harding, G.L., Zhiqiang, Y., Mackey, D.W., 1985, Heat Extraction Efficiency of a Concentric Glass Tubular Evacuated Collector , *Solar Energy*, vol. 35, no. 1: p. 71–79.

Incropera F.P., Dewitt, D.P., Bergman, T.L., Lavine, A.S., 2007, Fundamentals of Heat and Mass Transfer, John Wiley & Sons, Inc., New Jersey.

Liang, R., Ma, L., Zhang, J., Zhao, D., 2011, Theoretical and experimental investigation of the filled type evacuated tube solar collector with U-tube, *Solar Energy*, vol. 85, no. 1: 1735–1744.

Ma, L., Lu, Z., Zhang, J., Liang, R., 2010, Thermal performance analysis of the glass evacuated tube solar collector with U-tube, *Building and Environment*, vol. 45, no. 1: p. 1959-1967.

Rabl, A., 1975,Comparison of Solar Concentrators, *Solar Energy*, vol. 18, no. 1: p. 93-111.

Rabl, A., 1976, Optical and thermal properties of compound parabolic concentrators, *Solar Energy*, vol. 18, no. 1: p. 497-511.

Soriga, I., Neaga, C., 2012, Thermal analysis of a linear Fresnel lens solar collector with black body cavity receiver, *U.P.B. Sci. Bull., Series D*, vol. 74, no. 4, ISSN 1454-2358.

Zamboiln, E., Del Col, D., 2010, Experimental analysis of thermal performance of flat plate and evacuated tube solar collectors in stationary standard and daily conditions, *Solar Energy*, vol. 84, no. 1: p. 1382–1396.

Zamboiln, E., Del Col, D., 2012, An improved procedure for the experimental characterization of optical efficiency in evacuated tube solar collectors, *Renewable Energy*, vol. 43, no. 1: p. 37-46.

ACKNOWLEDGEMENTS

The authors of this work would like to thank the European Union's Erasmus Mundus Programme, Action 2 Lot 1 Fatima Al-Fihri Scholarship, for the financial support. UNISINOS (University of Vale do Rio dos Sinos - Brazil) and CAPES (Coordenação de Aperfeiçoamento de Pessoal de Nível Superior – Brazil) are also acknowledged for the financial support through the research project BEX 2614/13-8.